

Analysis of Cutting Fluid Jet Impingement on a Flat Surface via Computational Fluid Dynamics

Y. K. Siow
S. L. Yang
J. W. Sutherland

Department of Mechanical Engineering-Engineering Mechanis
Michigan Technological University

ABSTRACT

Cutting Fluid mist produced during machining operations is receiving increased attention by industry because of its adverse health effects. Thus, it is desired to obtain a fundamental understanding of the mechanisms that underlie mist formation. This knowledge can be used as a tool to design machining processes or systems that reduce the formation of cutting fluid mist and hence, the health hazard to which workers are exposed. Computational Fluid Dynamics is applied to investigate the problem, and a parametric study is performed to analyze the behavior of a cutting fluid when it impinges on a solid surface. A second-order, high-resolution Total Variation Diminishing (TVD) numerical scheme is incorporated to capture high velocity gradients. The results show that the TVD scheme can resolve free surface distortions and some fluid breakups. Validation is achieved by graphically comparing numerical results to a set of experimentally obtained images. The CFD analysis and experimental work indicate that the distance between the fluid nozzle and the work surface is the most critical variable in terms of mist formation.

INTRODUCTION

Metalworking fluids, or cutting fluids, are widely used in many machining operations. The primary functions of cutting fluids are cooling, lubricating, and flushing away chips. One of the principal concerns associated with cutting fluid use is the health effects that cutting fluid mist can cause. Unfortunately, mist is often produced as the cutting fluid impinges on the workpiece, particularly those rotating at high speeds. Previous industrial hygiene studies have revealed that cutting fluid

mist is a primary cause of work place illness [1] as well as detrimental effects on the environment [2].

Broadly, mist is an aerosol that contains liquid particles of diameters 20 μm and smaller. Droplet sizes 2.5 μm in diameter and below are especially hazardous to human lungs and respiratory system, since these ultra-fine particles can travel deep into the human respiratory tract. Once deposited in the airways and lungs, the oil particles can cause the narrowing of airways [3] and dysfunction or even cancer in other organs, such as the heart, pancreas, and prostate [4]. Besides the potential health hazard through inhalation, cutting fluid mist can also cause diseases through skin exposure. Folliculitis, oil acne, skin allergy and eye irritation are among the disorders that oil mist can cause. Therefore, in order to reduce the undesirable health effects of the mist to a minimum level, a thorough understanding of the physics and underlying mechanisms of mist formation is essential.

In most industrial applications where cutting fluid is used, mist is most prone to being produced via direct impingement (more commonly referred to as "atomization") of the fluid jet onto a rotating workpiece. The rotational motion of the fluid enhances the rapid growth of instability within the fluid film; as a result, tiny droplets are produced at relatively high rates. Cutting fluid impingement on surfaces of geometry other than rotating cylinders can also generate considerable amount of mist. To grasp the fundamental knowledge of mist formation mechanisms, the simplest geometry -- a flat surface, will be the focus of the present analysis.

Besides atomization, mist can also form via vaporization/condensation effect of cutting fluid. During machining processes, the

cutting zone often reaches high temperatures. When cutting fluid enters the vicinity of this region, the high temperature gradient may cause the fluid to vaporize. The vapor, when cooled in the surrounding air, will condense and eventually form mist.

Most of the research efforts in the area of droplet and ligament formation have been devoted to experimental observations. These include the breakdown of liquid jets and sheets in the air, and splashing of liquid drops into a deep pool of liquid or on solid surfaces. Research dated as far back as the late nineteenth century has investigated liquid jet instability and drop formation. In 1878, Rayleigh [5] attributed the instability to wave propagation on the free surface of a jet subject to a small initial perturbation. In the early twentieth century, Worthington [6,7] examined a series of photographs of liquid drops impacting on a wet or dry solid surface. Levin [8] also conducted a photographic experiment to study the behavior of a liquid drop when impacting on a flat surface. He observed that the impacted drop radially forms a liquid layer that contains many “crowns” that vary in diameter. He also related the effects of impact velocity to the crown size, crown height, and the time scale on which splashing occurs -- generally on the order of 10^{-4} seconds.

Several researchers, such as Hoyt and Taylor [9] and Spangler et al. [10], have investigated disintegration of liquid sheets where the growth of capillary waves and Kelvin-Helmholtz instability are the prevailing mechanisms. Errico [11] conducted an experimental study on splashing due to interactions between a liquid jet and a stationary solid surface. He concluded that the jet velocity, jet surface shape, and the distance between the nozzle and the solid surface had significant impact on the onset of splashing. His experiments indicated that no splashing occurred when the jet surface was smooth. This further demonstrates the effects of the growth of perturbation and instability of waves. Lienhard et al. [12] experimentally studied the splattering and heat transfer of a liquid jet impinging on a solid flat surface. The amount of the splattered droplets was found to be related to the magnitude of perturbation on the liquid jet, as well as the distance of nozzle to the solid surface. These findings agree well with the conclusions Errico [11] has made.

Gunter [13] performed a series of experiments to investigate the significant factors that influence cutting fluid mist formation in the turning process. Figure 1 shows a partial setup of his experiment where a jet of cutting fluid impinges on a rotating workpiece. He concluded that the spindle speed, as well as its interaction with other process conditions, has the most significant effect on the mist concentration level in the air.



Figure 1. Cutting Fluid Jet Impinging on a Rotating Workpiece

In addition to wave growth, fluid properties such as surface tension, viscosity, and density also have certain effects on drop formation. However, there has yet to be strong and convincing evidence on the role that these properties play in the formation of drops [14].

In a recent study by Yue et al. [15,16], an analytical model for the droplet diameter was developed based on experimental correlations. For mist formation due to atomization on a rotating cylindrical workpiece, there are two primary modes with which droplets can form: Drop mode and ligament mode. Drop mode takes place when the jet has a very low flow rate, and vice versa. The mean diameter of droplets via drop mode is given by

$$D = \frac{c}{\omega} \left(\frac{\sigma}{\rho R} \right)^{1/2} \dots (1)$$

which can be derived from the balance of surface tension and centrifugal forces. In Eq.(1), ω , R are the angular velocity and radius of the workpiece, and σ , ρ are the surface tension and density of the fluid, respectively. For ligament mode, the droplet diameter can be found from

$$D=1.23R\left(\frac{1}{K}\right)^{2/7}\left(\frac{\rho Q^2}{4\sigma R^3}\right)^{1/7}\left(\frac{\sigma}{\rho\alpha R^3}\right)^{2/7}\dots(2)$$

where Q is the volume flow rate of the cutting fluid, and K is the wave number which can be determined from the following relation:

$$We=K^2\left[3+(8K-3)S_i\left(1+\sqrt{1+\frac{1}{KS_i}}\right)\right]\dots(3)$$

The dimensionless numbers, We and S_i , are the Weber number and stability number, respectively.

It is obvious that the above expressions are obtained from experimental correlations. This posts some limitations to the models, since the resulting equations are dependent upon the experimental conditions and parameters, which may vary on a case-to-case basis. Therefore, a more robust technique is necessary to describe in full the conditions at which droplets/ligaments are formed, as well as the diameters and perhaps the concentrations of the mist. One such technique is Computational Fluid Dynamics, or CFD, where the fluid flow is obtained by solving the Navier-Stokes (N-S) equations in a discretized multidimensional domain. The effects of ligament formation, droplet breakup/coalescence, and turbulence is achieved by adding sub-models to the N-S equations.

Although CFD has been used with success in a variety of situations, such as aerospace, automotive, and environmental applications, it has yet to be applied in the area of cutting fluid mist formation. In particular, little attention has been paid in the case of cutting fluid impinging on a flat surface, using CFD techniques. In this study, a CFD simulation was conducted to study the behavior of a cutting fluid stream ejected from a nozzle, and impinging on either a stationary or a moving flat plate. Fluid jet velocity, plate velocity, and the nozzle height measured from the plate, were among the parameters to be examined. A computer code, RIPPLE [17], was employed in the simulations. In order to capture the large gradients and improve the resolution of free surface distortions, a second-order Total Variation Diminishing (TVD) scheme was incorporated for the computation of momentum advection. Validation of the results was obtained by comparing them with a series of experimentally obtained images, as well as with the simulated results from

RIPPLE's standard van Leer scheme for the momentum advection calculation.

CFD SIMULATIONS

Process Geometry

A cutting fluid stream impinging on a flat plate was examined. A parametric study was carried out to investigate several different scenarios. A two-level factorial (2^k) experimental design was employed to this parametric study. There were three variables, namely the plate velocity, jet velocity, and nozzle height measured vertically from the plate. Each variable was assigned two levels: high and low.

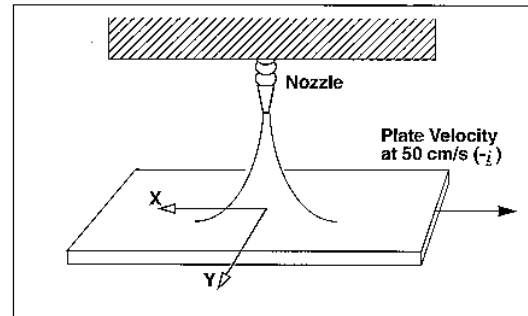


Figure 2. Orientation of Problem Geometry

For the nozzle height, either 8 cm (low level) or 15 cm (high level) was used. The nozzle, 0.75 cm in diameter, was placed above the flat plate. Cutting fluid (density $\rho = 994 \text{ kg/m}^3$, surface tension $\sigma = 0.026 \text{ N/m}$, kinematic viscosity $\nu = 1 \times 10^{-6} \text{ m}^2/\text{s}$) was ejected from the nozzle at either 1.5 m/s (low level) or 2.0 m/s (high level). The flat plate was either stationary (low level) or moving at 0.5 m/s (high level) in the $-x$ -direction, as indicated in Figure 2. Table 1 summarizes the cases described above.

Table 1: Cases For Parametric Study

	Plate Velocity (cm/s)	Jet Velocity (cm/s)	Nozzle Height (cm)
Case 1	0	150	8
Case 2	50	150	8
Case 3	0	200	8
Case 4	50	200	8
Case 5	0	150	15
Case 6	50	150	15
Case 7	0	200	15
Case 8	50	200	15

CFD Modeling

The situation where a fluid jet impinges on moving surface was described using the CFD code, RIPPLE. RIPPLE is a 2-D, Eulerian hydrocode that can solve transient and incompressible fluid flows with free surfaces. A volume-of-fluid (VOF) technique is used to resolve the free surfaces, and surface tension is modeled using a continuum surface force (CSF). The fluid flow solution is obtained by a two-step projection method. The first step involves solving the momentum equation without the pressure gradient. This momentum advection is approximated by a second-order upwind scheme of van Leer [18]. In the second step, the pressure term is combined with the continuity equation to form the pressure Poisson equation (PPE). This equation is then solved by employing an incomplete Cholesky conjugate gradient (ICCG) technique.

Due to the presence of free surfaces, and hence large gradients and discontinuities in the flow field, a high-resolution, spatially second-order, symmetric Total Variation Diminishing (TVD) scheme has been incorporated into RIPPLE, as an attempt to improve the solution of momentum advection. A particular form of the scheme, to be discussed below, was implemented to replace RIPPLE's original van Leer scheme.

High-resolution and higher-order TVD schemes are known to possess the ability to capture and resolve sharp interfaces and discontinuities in the flow field, such as a free surface. Under the constraint of the scheme, the total variation of the solution does not increase with time. This reinforces a physically reasonable solution [19].

The Governing Equations

RIPPLE solves for the continuity and momentum equations:

$$\nabla \cdot \vec{V} = 0 \dots (4)$$

$$\frac{\partial \vec{V}}{\partial t} + \nabla \cdot (\vec{V}\vec{V}) = -\frac{1}{\rho} \nabla p + \frac{1}{\rho} \nabla \cdot \vec{\tau} + \vec{g} + \frac{1}{\rho} \vec{F}_b \dots (5)$$

where F_b is the body force induced by the presence of free surfaces. In solving for the velocity field due to convection alone, i.e., the

momentum advection, Eq. (5) is written in conservative form as

$$\frac{\partial \vec{V}}{\partial t} = -\nabla \cdot (\vec{V}\vec{V}) \dots (6)$$

The x-component is therefore

$$\frac{\partial u}{\partial t} = -\nabla \cdot (u\vec{V}) = -\frac{\partial u^2}{\partial x} - \frac{\partial uv}{\partial y} \dots (7)$$

The Momentum Advection Solution with TVD

$$u_{i+\frac{1}{2},j}^{n+1} = u_{i+\frac{1}{2},j}^n - \Delta t \left(\frac{f_{i+1,j}^*}{\Delta x_{i+1,j}} - \frac{f_{i,j}^*}{\Delta x_{i,j}} \right) - \Delta t \left(\frac{g_{i,j+1}^*}{\Delta y_{i,j+1}} - \frac{g_{i,j}^*}{\Delta y_{i,j}} \right) \dots (8)$$

The grid system in RIPPLE is fully staggered, with momentum control volume centered at cell faces (Figure 3). Eq. (7) is then discretized and cast into a model of TVD scheme by Yee [20] and Yang et al. [21] for incompressible flow:

where

$$f_{i+1,j}^* = \frac{1}{2} [(F_{i+\frac{3}{2},j} + F_{i+\frac{1}{2},j}) - |a_{i+1,j}| (\Delta_{i+1,j} u - \hat{Q}_{i+1,j})] \dots (9)$$

and

$$g_{i,j+1}^* = \frac{1}{2} [(G_{i,j+\frac{3}{2}} + G_{i,j+\frac{1}{2}}) - |b_{i,j+1}| (\Delta_{i,j+1} v - \hat{Q}_{i,j+1})] \dots (10)$$

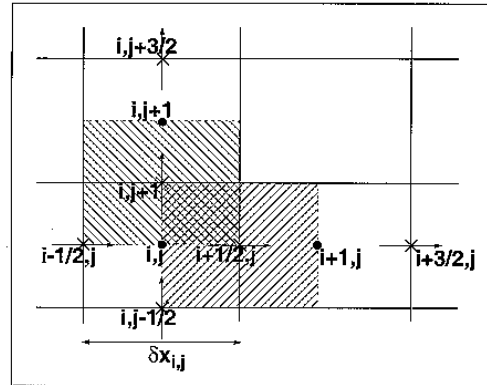


Figure 3. Momentum Control Volumes

The numerical fluxing terms F and G are modeled as

$$F_{i+\frac{3}{2},j} = (u_{i+\frac{3}{2},j})^2 \dots (11)$$

and

$$G_{i,j+\frac{3}{2}} = (u_{i,j+\frac{3}{2}})(v_{i,j+\frac{3}{2}}) \dots (12)$$

respectively, where the x-component velocity centered at cell faces is given by

$$u_{i,j+\frac{3}{2}} = \frac{\delta y_{i,j+1} u_{i,j+2} + \delta y_{i,j+2} u_{i,j+1}}{\delta y_{i,j+1} + \delta y_{i,j+2}} \dots (13)$$

Here, the velocity $u_{i,j+1}$ is a simple arithmetic average, given by

$$u_{i,j+1} = \frac{1}{2} (u_{i-\frac{1}{2},j+1} + u_{i+\frac{1}{2},j+1}) \dots (14)$$

The terms a and b are the characteristic speeds, i.e.,

$$\begin{aligned} a_{i+1,j} &= (\partial F / \partial u) |_{u_{i+1,j}} \\ b_{i,j+1} &= (\partial G / \partial u) |_{v_{i,j+1}} \dots (15) \end{aligned}$$

The notation “ u ” is defined such that

$$\Delta_{i+1,j} u = u_{i+\frac{3}{2},j} - u_{i+\frac{1}{2},j} \dots (16)$$

Finally, the “correction term” \hat{Q} is chosen (among several choices) as

$$\begin{aligned} &+ \min \text{mod}(\Delta_{i+1,j} u, \Delta_{i+2,j} u) - \Delta_{i+1,j} u \\ \hat{Q}_{i+1,j} &= \min \text{mod}(\Delta_{i,j} u, \Delta_{i+1,j} u) - \Delta_{i+1,j} u \dots (17) \end{aligned}$$

where

$$\min \text{mod}(x, y) = \text{sign}(x) \max(0, \min(|x|, y \cdot \text{sign}(x))) \dots (18)$$

All the above expressions for the y-component velocity can be similarly defined.

The Computational Mesh

The mesh employed in the simulation consists of a grid of 72x72 points. Two geometries were used, as shown in Figure 4. To insure the quality of the computational mesh, a grid dependency test was performed for Case 8 using the TVD scheme with a coarser grid (34x34 grid points) and a finer grid (100x100 grid points). The results for the dense grid agreed with the result for the 72x72 grid, while the coarse grid results differed substantially from the other grid results. Therefore, the grid used in current study can be concluded as appropriate.

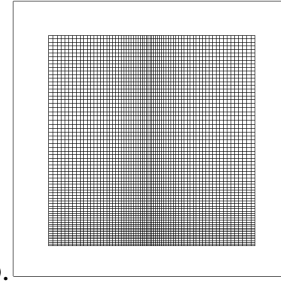
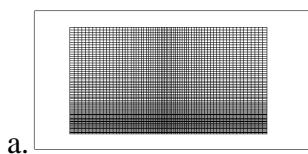


Figure 4. Computational Mesh for (a) Cases 1-4, 15cm x 8cm, (b) Cases 5-8, 15cm x 15cm

RESULTS AND DISCUSSIONS

Figure 5 shows the calculated results with the van Leer scheme for Cases 2, 4, 6, and 8. It can be clearly seen that the scheme did not predict any turbulent fluid flows, nor did it resolve any visible free surface distortions. A comparison with the images, shown in Figure 6 for the same cases, proves that the van Leer scheme did not capture any of the disturbances on the fluid’s free surface.

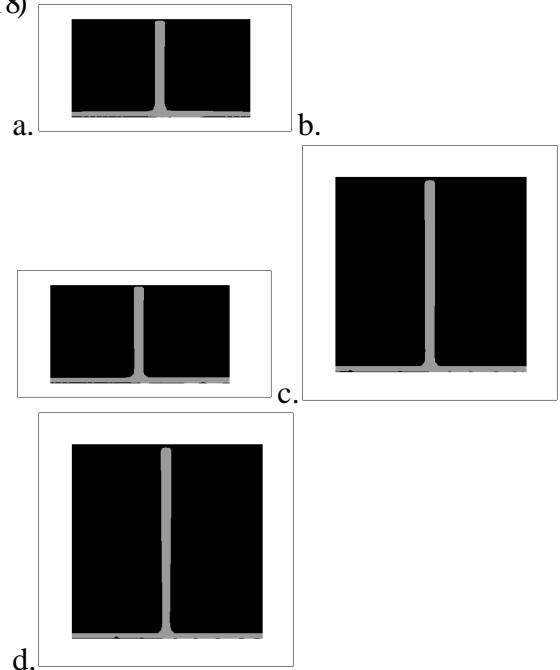


Figure 5. Van Leer Results: a) Case 2, b) Case 4, c) Case 6, d) Case 8

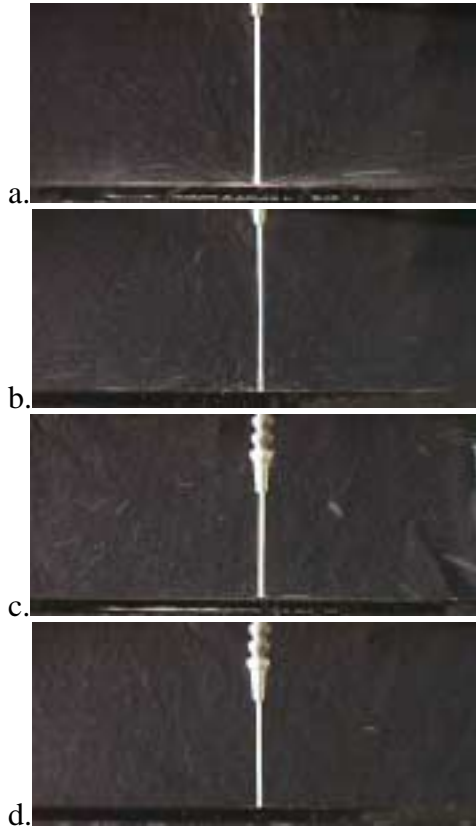


Figure 6. Images: a) Case 2, b) Case 4, c) Case 6, d) Case 8

The TVD results, on the other hand, present a quite different scenario from the van Leer calculations, as Figure 7 shows. A close look at the results suggests that the TVD scheme is capable of predicting more vigorous fluid flow than van Leer scheme, particularly in the moving-plate cases. The van Leer results show little effects of jet speed, plate speed, or jet height; the fluid jet in all the cases maintains a smooth profile. The TVD calculations, on the other hand, compare more closely to the images. A considerably high level of turbulence is present in all cases. Both the images and the TVD results show small ripples on the plate in Case 6. The TVD calculation of Case 8 shows some splattering and droplets that are also present in the image.

Velocity vectors were plotted for Case 8, as shown in Figure 8. It is obvious that with van Leer scheme, the flow of fluid is much more subdued than with TVD.

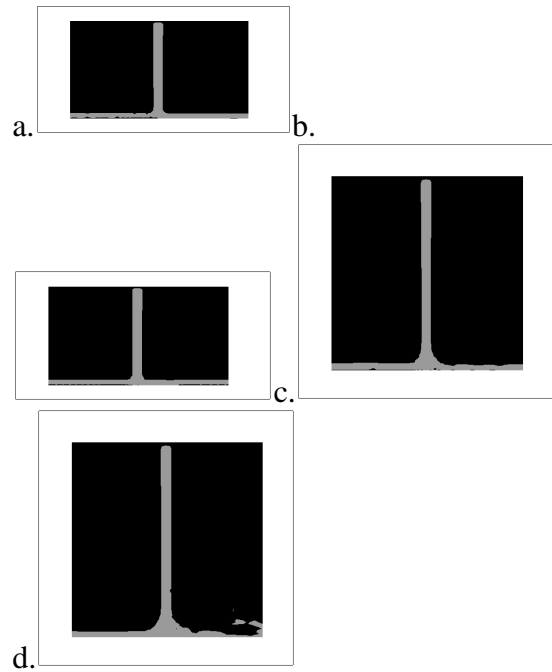


Figure 7. TVD Results: a) Case 2, b) Case 4, c) Case 6, d) Case 8

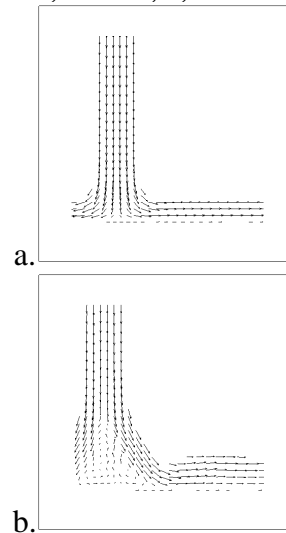


Figure 8. Velocity Vector Plots for Case 8: a) Van Leer, b) TVD

In the TVD result, a circulation zone appears within the impingement area. This implies a more “energetic” jet flow and a more accurate prediction of perturbation that is induced by the interaction between the jet and the moving plate. The TVD-vectors on the plate near the impingement zone appear to exhibit upward motion, which suggests that the fluid tends to bounce and hence, splatter after impingement.

Some consistencies are observed in both experiment and simulation. First, the nozzle height plays the most significant role among all three parameters. As the nozzle is brought closer to the flat plate, much less

c.

d.

disturbances are introduced, since the jet surface is able to maintain its smoothness in such short distance. This phenomenon further validates the observation by Errico [11]. Second, the relatively slow moving plate does not affect the flow characteristics observed in the stationary-plate cases. The presence of instability is attributed to the jet alone.

In addition to the eight cases above, a series of simulation study was performed for a plate moving at 2.0 m/s, the results of which are shown in Figures 9 and 10. As before, the TVD scheme produced much more turbulent flow field than its counterpart. Fluid circulates and accumulates on one side of the jet, and in some cases, splashes as high as the height of the jet itself. In reality, those splattered fluid may be more diverse and may contain a large number of fine droplets, which was not predicted by both schemes. However, with TVD method it appears that the general behavior of fluid flow can be captured with substantial confidence. A droplet-breakup model, combined with the TVD scheme used here, may be able to resolve these splattering phenomena.

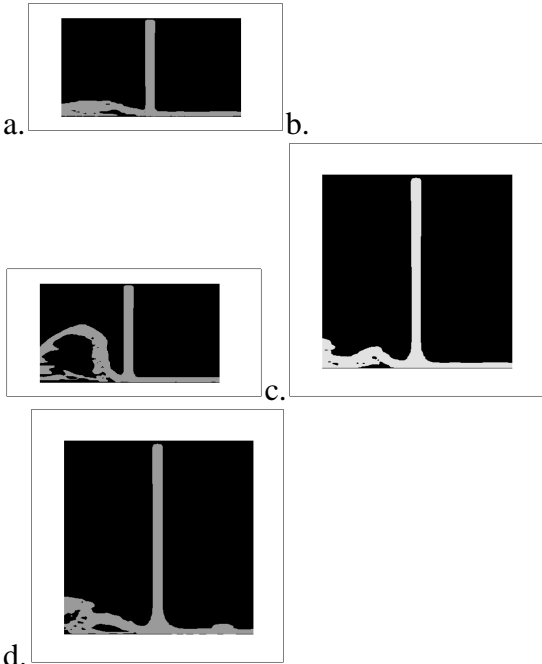


Figure 9. TVD: Moving Plate at 2.0 m/s:
a) Case 2, b) Case 4, c) Case 6, d) Case8

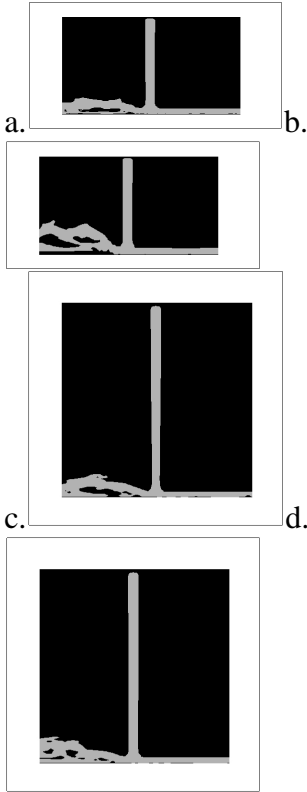


Figure 10. Van Leer: Moving Plate at 2.0 m/s:
a) Case 2, b) Case 4, c) Case 6, d) Case8

CONCLUSIONS

A numerical study of a cutting fluid jet impinging on a stationary/moving flat plate was conducted. Results from the different momentum advection schemes were compared, and validation was achieved by comparing the simulated results with experimentally obtained images. This study is summarized as follows:

- Computational Fluid Dynamics (CFD) was successfully applied to simulate a cutting fluid stream impinging on a moving flat plate
- A Total Variation Diminishing (TVD) scheme was incorporated into the calculation of momentum advection
- A parametric study was performed to determine the significant factors contributing to cutting fluid mist formation

It was shown that for the velocities used in the experiments, the high-resolution numerical scheme of TVD was able to predict the general behavior of the fluid flow more closely to that of the experimentally obtained images than the original van Leer method. Based on the above

observations and comparison of results, the following conclusions may be drawn:

- The closer the nozzle is to the flat plate, the less likely the cutting fluid will splatter
- The TVD scheme is superior to the van Leer method in resolving high velocity gradients and discontinuities

This study has established a ground work for the pursuit of a thorough understanding of the mechanisms underlying cutting fluid mist formation. The use of high-resolution, high-order momentum advection schemes, such as TVD, will improve the results as this study has shown. Improvements may also be achieved through a three-dimensional analysis, a numerical modeling scheme capable of resolving fine droplets/ligaments, and multicomponent modeling of the problem.

ACKNOWLEDGEMENT

The authors would like to thank Dr. Douglas Kothe at the Los Alamos National Laboratory for providing the RIPPLE computer code. This research was supported under the PECASE (Presidential Early Career Award for Scientists and Engineers) Award No. DMI-9628984.

REFERENCES

1. Bennett, E. O., and Bennett, D. L., Minimizing Human Exposure to Chemicals in Metalworking Fluids, *Lubrication Engineering*, Vol. 43, No. 3, 1987, pp. 167-175.
2. Sutherland, J. W., Yue, Y., Zheng, Y., Gunter, K. L., Cao, T., and Zhang, W., Evaluation of Environmental Effects and Process Impact of Cutting Fluids, *Proceedings of the 1998 NSF Design & Manufacturing Grantees Conference*, 1998, pp. 369-370.
3. Kennedy, S. M., Acute Pulmonary Responses Among Automobile Workers Exposed to Aerosols of Machining Fluids, *American Journal of Industrial Medicine*, Vol. 15, 1989, pp. 627-641.
4. Raynor, P., Cooper, S., and Leith, D., Evaporation of Polydisperse Multicomponent Oil Droplets, *American Industrial Hygiene Association Journal*, Vol. 57, No. 12, 1996, pp. 1128-1136.
5. Rayleigh, Lord, On the Instability of Jets, *Proc. London Math. Soc.*, Vol. 10, 1878, pp. 4-13.
6. Worthington, A. M., On the Forms Assumed by Drops of Liquids Falling Vertically on a Horizontal Plate, *Proc. Roy. Soc.*, Vol. 25, 1877, pp. 261-271.
7. Worthington, A. M., *A Study of Splashes*, MacMillan, New York, 1963.
8. Levin, Z., Splashing of Water Drops: A Study of the Hydrodynamics and Charge Separation, Ph.D. Dissertation, University of Washington, 1970.
9. Hoyt, J. W., and Taylor, J. J., Waves on Water Jets, *Journal of Fluid Mechanics*, Vol. 83, No. 1, 1977, pp. 119-127.
10. Spangler, C. A., Hilbing, J. H., and Heister, S. D., Nonlinear Modeling of Jet Atomization in the Wind-induced Regime, *Physics of Fluids*, Vol. 7, No. 5, May 1995, pp. 964-971.
11. Errico, M., A Study of Interaction of Liquid Jets with Solid Surfaces, Ph.D. Dissertation, University of California at San Diego, 1986.
12. Lienhard, J. H. V., Liu, X., and Gabour, L. A., Splattering and Heat Transfer During Impingement of a Turbulent Liquid Jet, *ASME, Heat Transfer Division*, Vol. 168, July 1991, pp. 51-60.
13. Gunter, K. L., An Experimental Investigation of Cutting Fluid Mist Formation via Atomization in the Turning Process, MS. Thesis, Michigan Technological University, 1999.
14. Chigier, N. A., The Physics of Atomization, *ICLASS-91*, Plenary Lecture, Paper A, Gaithersburg, MD, July 1991, pp. 1-15.
15. Yue, Y., Gunter, K. L., Michalek, D. J., and Sutherland, J. W., An Examination of Cutting Fluid Mist

- Formation in Turning, *Transactions of NAMRI/SME*, Vol. 27, 1999, pp. 221-226.
16. Yue, Y., Sutherland, J. W., and Olson, W. W., Cutting Fluid Mist Formation in Machining via Atomization Mechanisms, *Proceedings of the ASME Design for Manufacturability Symposium*, 1996, pp. 37-46.
 17. Kothe, D. B., Mjolsness, R. C., and Torrey, M. D., RIPPLE: A Computer Program for Incompressible Flows with Free Surfaces, LA-12007-MS, Los Alamos National Laboratory, 1991.
 18. Van Leer, B., Towards the Ultimate Conservative Difference Scheme. V. A Second-order Sequel to Godunov's Method, *Journal of Computational Physics*, Vol. 32, 1979, pp. 101-136.
 19. Anderson, J. D., *Computational Fluid Dynamics: The Basics with Applications*, 1st ed., McGraw- Hill, New York, 1995, pp. 499-510.
 20. Yee, H. C., Upwind and Symmetric Shock- Capturing Schemes, NASA TM-89464, 1987.
 21. Yang, S. L., Chang, Y. L., and Arici, O., Incompressible Navier-Stokes Computation of the NREL Airfoils Using a Symmetric Total Variational Diminishing Scheme, *Transactions of the ASME*, Vol. 116, November 1994, pp. 174-182.
 - 22.